CHALMERS | UNIVERSITY OF GOTHENBURG

PREPRINT 2014:14

Inverse Eigenvalue Problems in the Theory of Weakly Guiding Step-Index Optical Fibres

E. KARCHEVSKII
A. SPIRIDINOV
A. REPINA
L. BEILINA

Department of Mathematical Sciences
Division of Mathematics
CHALMERS UNIVERSITY OF TECHNOLOGY
UNIVERSITY OF GOTHENBURG
Gothenburg Sweden 2014

Preprint 2014:14

Inverse Eigenvalue Problems in the Theory of Weakly Guiding Step-Index Optical Fibres

E. Karchevskii, A. Spiridinov, A. Repina, L. Beilina

Department of Mathematical Sciences
Division of Mathematics
Chalmers University of Technology and University of Gothenburg
SE-412 96 Gothenburg, Sweden
Gothenburg, August 2014

Preprint 2014:14
ISSN 1652-9715

Matematiska vetenskaper
Göteborg 2014

Inverse Eigenvalue Problems in the Theory of Weakly Guiding Step-Index Optical Fibers

Karchevskii E., Spiridonov A., Repina A.
Kazan Federal University, Kremlevskaya 18, 420008 Kazan, Russia; e-mail: ekarchev@yandex.ru
Beilina L.
Chalmers University of Technology and Gothenburg University, SE-42196 Gothenburg, Sweden;
e-mail: larisa@chalmers.se

We formulate three inverse spectral problems and present new methods for calculation of dielectric constants of core and cladding of optical fibers using propagation constants measurements. We prove that our three inverse problems are well-posed. We also show that for unique and stable reconstruction of one dielectric constant of core or of cladding it is enough to measure propagation constant of fundamental mode only at one frequency. For reconstruction of both dielectric constants of core and of cladding it is enough to measure propagation constants at two frequencies. Our numerical algorithms are based on approximate solution of a nonlinear nonselfadjoint eigenvalue problem for a system of weakly singular integral equations. Integral operators are approximated by a spline-collocation method. We propose to use the singular value decomposition (SVD) to obtain an initial approximation to eigenvalues for the matrix in the spline-collocation method. For the computations of three test inverse spectral problems we use parallel computing technologies (OpenMP and MPI) to show performance and efficiency of our calculations.

1 Introduction

There are many non-destructive material characterization techniques for obtaining permittivity of dielectric materials in closed waveguides (see a short review of recent results in [1]). Particularly, permittivity determination problems from measurements of propagation constants were investigated firstly for closed rectangular waveguides in [2]. For open dielectric waveguides of arbitrary cross section such problems can be set up as inverse eigenvalue problems [3] of the theory of optical waveguides [4]. Inverse eigenvalue problems arise in a remarkable variety of applications, including system and control theory, geophysics, molecular spectroscopy, particle physics, structure analysis, and so on. An inverse eigenvalue problem concerns the reconstruction of a physical system from prescribed spectral data. The involved spectral data may consist of the complete or only partial information of eigenvalues or eigenvectors.

In this work we formulate and solve new inverse spectral problems on reconstruction of dielectric constants of core and cladding of optical fibers using propagation constants measurements. The statements of problems are based on integral formulations. Two mathematical models of optical waveguides were investigated in details by integral equation methods: step-index waveguides [5]–[8] and waveguides without a sharp boundary [9]–[11]. A review of modern results in this field is given in [12]. We use a mathematical model of a weakly-guiding step-index arbitrarily shaped optical fiber and formulate three inverse spectral problems. Then we present new numerical algorithms for dielectric constants calculation based on an approximate solution of a nonlinear nonselfadjoint eigenvalue problem for a system of weakly singular integral equations. Any information on specific values of eigenfunctions is not required. In our algorithms it is enough to know that the fundamental mode is excited, and then to measure its propagation constant for one or for two frequencies. We prove that it is enough to measure propagation constants of fundamental eigenmode at two distinct frequencies for unique and stable reconstruction of both unknown dielectric constants of core and cladding of the fiber. For reconstruction of the core's permittivity it is enough to measure the propagation constant only at one frequency. The same result is obtained for reconstruction of the cladding's permittivity.

Our conclusions are based on the analysis of the mathematical model and results of numerical experiments. Integral operators were approximated by a spline-collocation method proposed in [8]. The main difficulty with practical solution of obtained finite-dimensional nonlinear spectral problem are calculations of good initial approximations for eigenvalues. Usually initial approximations are chosen by a physical intuition using a prior information on solutions. If we solve inverse problems

then we may not have an accurate prior information on solutions. Therefore, we investigate properties of the spline-collocation method's matrix as a function of spectral and non-spectral parameters. For each given point in an investigated domain of parameters we calculate the condition number of matrix. If for given non-spectral parameter a spectral parameter is equal to a nonlinear eigenvalue of matrix, then the condition number is equal to infinity. Therefore, the numbers for which the condition number is big enough are good approximations for eigenvalues.

The condition number is calculated by singular value decomposition method (SVD). The calculations are based on unitary transformations of matrix and therefore are stable. However, if the condition number is calculated for a wide range of parameters, then a large amount of calculations is needed. Kazan Federal University purchased a compact supercomputer APK-1M according to the program of university development. Now this supercomputer is a base of hardware of Kazan Laboratory of the Supercomputer Modeling. Kazan team are programming for this supercomputer and we have decided to investigate numerically the problem on calculations of good initial approximations for nonlinear eigenvalues. Using parallel computational technologies (OpenMP and MPI) we solved this problem directly and without any prior information.

2 Nonlinear eigenvalue problem for transverse wavenumbers

2.1 Statement of problem and properties of solutions

Let us consider an optical fiber as a regular cylindrical dielectric waveguide in a free space. The cross-section of the waveguide's core is a bounded domain Ω_i with a twice continuously differentiable boundary γ (see Fig. 1). The axis of the cylinder is parallel to the x_3-axis. Let $\Omega_e = \mathtt{R}^2 \setminus \overline{\Omega}_i$ be the unbounded domain of the cladding. Let the permittivity be prescribed as a positive piecewise constant function ε which is equal to a constant ε_∞ in the domain Ω_e and to a constant $\varepsilon_+ > \varepsilon_\infty$ in the domain Ω_i.

Eigenvalue problems of optical waveguide theory [4] are formulated on the base of the set of homogeneous Maxwell equations

$$\mathrm{rot}\mathcal{E} = -\mu_0 \frac{\partial \mathcal{H}}{\partial t}, \quad \mathrm{rot}\mathcal{H} = \varepsilon_0 \varepsilon \frac{\partial \mathcal{E}}{\partial t}. \qquad (1)$$

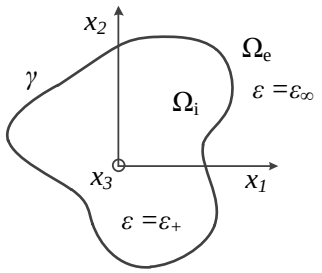

Figure 1: The cross-section of a cylindrical dielectric waveguide in a free-space

Here, $\mathcal{E}$ and $\mathcal{H}$ are electric and magnetic field vectors; ε_0 and μ_0 are the free-space dielectric and magnetic constants. Nontrivial solutions of set (1) which have the form

$$\begin{bmatrix} \mathcal{E} \\ \mathcal{H} \end{bmatrix}(x, x_3, t) = \mathrm{Re}\left(\begin{bmatrix} \mathrm{E} \\ \mathrm{H} \end{bmatrix}(x) e^{i(\beta x_3 - \omega t)} \right) \qquad (2)$$

are called the eigenmodes of the waveguide. Here, positive ω is the radian frequency, β is the propagation constant, E and H are complex amplitudes of $\mathcal{E}$ and $\mathcal{H}$, $x = (x_1, x_2)$.

In forward eigenvalue problems the permittivity is known and it is necessary to calculate longitudinal wavenumbers $k = \omega\sqrt{\varepsilon_0 \mu_0}$ and propagation constants β such that there exist eigenmodes. The eigenmodes have to satisfy to a transparency condition at the boundary γ and to a condition at infinity.

In inverse eigenvalue problems it is necessary to reconstruct the unknown permittivity ε by some information on natural eigenmodes which exists for some eigenvalues k and β. The main question is how many observations of natural eigenmodes are enough for unique and stable reconstruction of the permittivity.

The domain Ω_e is unbounded. Therefore, it is necessary to formulate a condition at infinity for complex amplitudes E and H of eigenmodes. Let us confine ourselves to the investigation of the surface modes only. The propagation constants β of surface modes are real and belong to the interval $G = (k\varepsilon_\infty, k\varepsilon_+)$. The amplitudes of surface modes satisfy to the following condition:

$$\begin{bmatrix} \mathrm{E} \\ \mathrm{H} \end{bmatrix} = e^{-\sigma r} O\left(\frac{1}{\sqrt{r}}\right), \quad r = |x| \to \infty. \qquad (3)$$

Here, $\sigma = \sqrt{\beta^2 - k^2 \varepsilon_\infty} > 0$ is the transverse wavenumber in the cladding.

Denote by $\chi = \sqrt{k^2\varepsilon_+ - \beta^2}$ the transverse wavenumber in the waveguide's core. Under the weakly guidance approximation [4] the original problem was reduced in [6] to the calculation of numbers χ and σ such that there exist nontrivial solutions $u = \mathrm{H}_1 = \mathrm{H}_2$ of Helmholtz equations

$$\Delta u + \chi^2 u = 0, \quad x \in \Omega_i, \tag{4}$$

$$\Delta u - \sigma^2 u = 0, \quad x \in \Omega_e, \tag{5}$$

which satisfy to the transparency conditions

$$u^+ = u^-, \quad \frac{\partial u^+}{\partial \nu} = \frac{\partial u^-}{\partial \nu}, \quad x \in \gamma. \tag{6}$$

Here, ν is the normal derivative on γ, u^- (respectively, u^+) is the limit value of a function u from the interior (respectively, the exterior) of γ.

Let us calculate nontrivial solutions u of problem (4)–(6) in the space of continuous and continuously differentiable in $\overline{\Omega}_i$ and $\overline{\Omega}_e$ and twice continuously differentiable in Ω_i and Ω_e functions, satisfying to condition

$$u = e^{-\sigma r} O\left(\frac{1}{\sqrt{r}}\right), \quad r = |x| \to \infty. \tag{7}$$

Denote by U described functional space.

Let $\sigma > 0$ be a given number. A nonzero function $u \in U$ is called an eigenfunction of the problem (4)–(6) corresponding to an real eigenvalue χ if relationships (4)–(6) hold.

The next theorem follows from results of [6].

Theorem 1. *For any $\sigma > 0$ the eigenvalues χ of problem (4)–(6) can be only positive isolated numbers. Each number χ depends continuously on σ.*

For waveguides of circular cross-section the analogous results about the localization of the surface modes spectrum and about the continuous dependence between the transverse wavenumbers σ and χ were obtained in [4]. The results of [4] were obtained only for waveguides of circular cross-section by the method of separation of variables. Theorem 1 generalizes the results of [4] to the case of an arbitrary smooth boundary.

The next theorem follows from results of [11] (see an illustration at Fig. 2).

Theorem 2. *The following statements hold:*

1. For any $\sigma > 0$ there exist the denumerable set of positive eigenvalues $\chi_i(\sigma)$, where $i = 1, 2, ...$, of a finite multiplicity with only cumulative point at infinity.

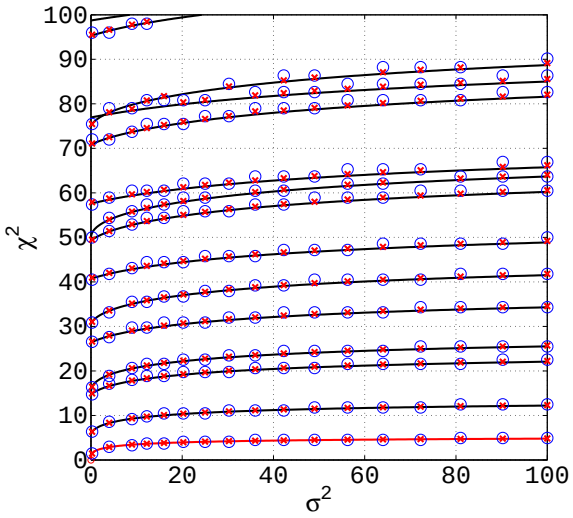

Figure 2: The plot of the computed by the spline-collocation method dispersion curves for surface eigenmodes of a weakly guiding dielectric waveguide of the circular cross-section. The exact solutions are plotted by solid lines. The solution for the fundamental mode is plotted by the bottom red solid line. Numerical solutions of the residual inverse iteration method are marked by red crosses. SVD's initial approximations to the numerical solutions are marked by blue circles.

2. For any $\sigma > 0$ the smallest eigenvalue $\chi_1(\sigma)$ is positive and simple (its multiplicity is equal to one), corresponding eigenfunction u_1 can be chosen as the positive function in the domain Ω_i.

3. $\chi_1(\sigma) \to 0$ at $\sigma \to 0$.

For a given $\sigma > 0$ the smallest eigenvalue $\chi_1(\sigma)$ and corresponding eigenfunction u_1 define the eigenmode which is called the fundamental mode (see the bottom curve plotted by the red solid line at Fig. 2). Thus, Theorem 2 states, particularly, that for any $\sigma > 0$ there exists exactly one fundamental mode.

To compute eigenmodes we use the representation of eigenfunctions of problem (4)–(6) in the form of single-layer potentials [13]:

$$u(x) = \int_\gamma \Phi(\chi; x, y) f(y) dl(y), \quad x \in \Omega_i, \tag{8}$$

$$u(x) = \int_\gamma \Psi(\sigma; x, y) g(y) dl(y), \quad x \in \Omega_e. \tag{9}$$

Here

$$\Phi(\chi;x,y)=\frac{i}{4}H_0^{(1)}(\chi|x-y|), \tag{10}$$

$$\Psi(\sigma;x,y)=\frac{1}{2\pi}K_0(\sigma|x-y|) \tag{11}$$

are the fundamental solutions of Helmholtz equations (4) and (5) correspondingly, $H_0^{(1)}(z)$ is Hankel function of the first kind, $K_0(z)$ is Macdonald function; unknown densities f and g belong to the Hölder space $C^{0,\alpha}(\gamma)$. Then f and g satisfy to the following system of boundary integral equations for $x\in\gamma$:

$$\mathcal{A}_{11}(\chi)f+\mathcal{A}_{12}(\sigma)g=0, \tag{12}$$

$$\mathcal{A}_{21}(\chi)f+\mathcal{A}_{22}(\sigma)g=0, \tag{13}$$

where

$$(\mathcal{A}_{11}(\chi)f)(x)=\int_\gamma\Phi(\chi;x,y)f(y)dl(y),$$

$$(\mathcal{A}_{12}(\sigma)g)(x)=-\int_\gamma\Psi(\sigma;x,y)g(y)dl(y),$$

$$(\mathcal{A}_{21}(\chi)f)(x)=\frac{1}{2}f(x)+\int_\gamma\frac{\partial\Phi(\chi;x,y)}{\partial\nu(x)}f(y)dl(y),$$

$$(\mathcal{A}_{22}(\sigma)g)(x)=\frac{1}{2}g(x)-\int_\gamma\frac{\partial\Psi(\sigma;x,y)}{\partial\nu(x)}g(y)dl(y).$$

Suppose that the boundary γ is parametrically defined by a function $r=r(t)$ of $t\in[0,2\pi]$ and this parametrization is regular. We consider functions from $C^{0,\alpha}(\gamma)$ and $C^{1,\alpha}(\gamma)$ as Hölder-continues and Hölder-continuously differentiable 2π-periodic functions of parameter t. Then for $x=x(t)\in\gamma$, where $t\in[0,2\pi]$, system (12), (13) is transformed to the following system of equations:

$$Lp_1+B_{11}(\chi,\sigma)p_1+B_{12}(\chi,\sigma)p_2=0, \tag{14}$$

$$p_2+B_{21}(\chi,\sigma)p_1+B_{22}(\chi,\sigma)p_2=0. \tag{15}$$

Here new unknown functions are defined as follows:

$$p_1(\tau)=(f(y)-g(y))|r'(\tau)|,\quad p_2(\tau)=f(y)+g(y),$$

$$y=y(\tau),\quad \tau\in[0,2\pi],$$

Integral operators are defined by the following relationships for $t\in[0,2\pi]$:

$$(Lp_1)(t)=-\frac{1}{2\pi}\int_0^{2\pi}\ln|\sin\frac{t-\tau}{2}|\,p_1(\tau)d\tau,$$

$$\left(B_{ij}(\chi,\sigma)p^{(j)}\right)(t)=\frac{1}{2\pi}\int_0^{2\pi}h_{ij}(\chi,\sigma;t,\tau)p^{(j)}(\tau)d\tau,$$

where

$$h_{11}(\chi,\sigma;t,\tau)=2\pi\left(G_{11}(\chi;t,\tau)+G_{12}(\sigma;t,\tau)\right),$$

$$h_{12}(\chi,\sigma;t,\tau)=$$

$$2\pi\left(G_{11}(\chi;t,\tau)-G_{12}(\sigma;t,\tau)\right)|r'(\tau)|,$$

$$h_{21}(\chi,\sigma;t,\tau)=4\pi\left(G_{21}(\chi;t,\tau)+G_{22}(\sigma;t,\tau)\right),$$

$$h_{22}(\chi,\sigma;t,\tau)=$$

$$4\pi\left(G_{21}(\chi;t,\tau)-G_{22}(\sigma;t,\tau)\right)|r'(\tau)|,$$

$$G_{11}(\chi;t,\tau)=\Phi(\chi;x,y)+\frac{1}{2\pi}\ln|\sin\frac{t-\tau}{2}|,$$

$$G_{12}(\sigma;t,\tau)=\Psi(\sigma;x,y)+\frac{1}{2\pi}\ln|\sin\frac{t-\tau}{2}|,$$

$$G_{21}(\chi;t,\tau)=\frac{\partial\Phi(\chi;x,y)}{\partial\nu(x)},$$

$$G_{22}(\sigma;t,\tau)=\frac{\partial\Psi(\sigma;x,y)}{\partial\nu(x)}.$$

The linear operator $L:C^{0,\alpha}(\gamma)\to C^{1,\alpha}(\gamma)$ is continuous and continuously invertible (for details see, for example, [6]). It was proved in [6] that for each $\chi>0$, $\sigma>0$ the linear operators

$$B_{21}(\chi,\sigma),\ B_{22}(\chi,\sigma):C^{0,\alpha}(\gamma)\to C^{0,\alpha}(\gamma),$$

$$B_{11}(\chi,\sigma),\ B_{12}(\chi,\sigma):C^{0,\alpha}(\gamma)\to C^{1,\alpha}(\gamma)$$

are compact. Therefore, the system (12), (13) is equivalent to the following Fredholm operator equation of the second kind:

$$A(\chi,\sigma)w=(I+B(\chi,\sigma))w=0, \tag{16}$$

where $w=(w_1,w_2)^T$,

$$w_1=Lp_1\in C^{1,\alpha}(\gamma),\quad w_2=p_2\in C^{0,\alpha}(\gamma),$$

the compact operator B acting in the Banach space $W=C^{1,\alpha}(\gamma)\times C^{0,\alpha}(\gamma)$ is defined as follows:

$$Bw=\begin{bmatrix}B_{11}L^{-1} & B_{12}\\ B_{21}L^{-1} & B_{22}\end{bmatrix}\begin{bmatrix}w_1\\ w_2\end{bmatrix}, \tag{17}$$

and I is the identical operator.

Let $\sigma>0$ be a given number. A nonzero element $w\in W$ is called an eigenfunction of the operator-valued function $A(\chi)$ corresponding to a characteristic value $\chi>0$, if equation (16) holds.

It follows from results of [6] that original problem (4)–(6) is spectrally equivalent to (16). Namely, the following theorem is true.

Theorem 3. *Let $\sigma > 0$ be a given number. The following statements hold.*

1. If a function w is the eigenfunction of the operator-valued function $A(\chi)$ corresponding to a characteristic value $\chi_0 > 0$, then the function u defined by equalities (8) *and* (9)*, where $\chi = \chi_0$,*

$$f = w_2/2 + L^{-1}w_1/(2|r'|),$$

$$g = w_2/2 - L^{-1}w_1/(2|r'|),$$

is the eigenfunction of problem (4)–(6) *corresponding to the eigenvalue χ_0.*

2. Each eigenfunction of problem (4)–(6) *corresponding to an eigenvalue $\chi_0 > 0$ can be represented in the form of single-layer potentials* (8) *and* (9) *with some Hölder-continuous densities f and g, respectively. At the same time the function*

$$w = (L((f-g)|r'|), f+g)$$

is the eigenfunction of the operator-valued function $A(\chi)$ corresponding to the characteristic value χ_0.

Let us formulate the nonlinear spectral problem for transverse wavenumbers by the following way. Suppose that the boundary γ of the waveguide's cross-section and the number $\sigma > 0$ are given. It is necessary to calculate all characteristic values χ of the operator-valued function $A(\chi)$ in some given interval.

2.2 Numerical method

A spline-collocation method was proposed in [8] for numerical calculations of characteristic values χ of the operator-valued function $A(\chi)$ for given σ such that the problem (16) for each fixed σ was reduced to a nonlinear finite-dimensional eigenvalue problem of the form

$$A_n(\chi)w_n = 0, \tag{18}$$

where n is the number of collocation points. For numerical solution of obtained nonlinear finite-dimensional eigenvalue problem we use the residual inverse iteration method [14].

Any iterative numerical method for computations of the nonlinear eigenvalues χ needs in good initial approximations for each given σ. Usually initial approximations are chosen by a physical intuition using a prior information on solutions. If we model fundamentally new types of waveguides, solve inverse problems, or investigate defects in fibers, then we may not have an accurate prior information on solutions.

In this case we can investigate spectral properties of the matrix $A_n(\chi)$ as a function of variable χ for each fixed σ. For each given point in an investigated domain of parameters χ and σ we calculate the condition number of matrix A_n:

$$\mathrm{cond}(A_n(\chi)) = \frac{\rho_1}{\rho_n}, \tag{19}$$

where ρ_1 and ρ_n are maximal and minimal singular values of matrix. If for given σ a number χ is equal to a nonlinear eigenvalue of $A_n(\chi)$, then the condition number is equal to infinity. Therefore, the numbers χ for which the condition number is big enough are good approximations for eigenvalues (see [15] as an example of analogous approach). Singular values are calculated by singular value decomposition method (SVD):

$$A_n(\chi) = USV, \quad S = \mathrm{diag}(\rho_1, \rho_2, ..., \rho_n), \tag{20}$$

where U, V are unitary matrices, S is a diagonal matrix, the singular numbers form S. The calculations are based on unitary transformations of the matrix A and therefore are stable.

In the next step for each σ in the investigated interval we use obtained initial approximations for numerical calculations of nonlinear eigenvalues χ by the residual inverse iteration method.

2.3 Numerical results

Let us describe numerical results obtained for nonlinear eigenvalue problem (16) for transverse wavenumbers. We compare our numerical results with the well-known exact solution for the circular waveguide obtained by the method of separation of variables (see, for example, [4]). At Fig. 2 we present some dispersion curves for surface eigenwaves of the circular waveguide. The exact solution is plotted by solid lines.

We started our numerical calculations with computations of initial approximations to nonlinear eigenvalues χ. We used SVD as was described in the end of subsection 2.2. Calculated initial approximations are marked at Fig. 2 by blue circles.

The blue circles are the initial approximations only. We used these initial approximations as start

points for the residual inverse iteration method. Using this iteration method for each given σ we solved numerically the finite-dimensional nonlinear eigenvalue problem (18) on eigenvalues χ by the iteration method. The numerical results are marked at Fig. 2 by red crosses.

Note here, that using previously calculated initial approximations we solved numerically this problem directly and without any prior physical information. The next our conclusion from the observation of Fig. 2 is that the initial approximations are good enough and we can use them in the majority of cases without iterative refinement of solutions.

3 Forward and inverse spectral problems

On the base of solution of nonlinear eigenvalue problem (16) for transverse wavenumbers we solve the forward and inverse spectral problems for weakly guiding step-index waveguides.

3.1 Forward spectral problem

Clearly, if for given σ the characteristic values χ of the operator-valued function $A(\chi)$ were calculated, and also if the permittivities ε_+, ε_∞ are known, then the longitudinal wavenumber k and the propagation constant β are calculated by the following explicit formulas:

$$k^2 = \frac{\sigma^2 + \chi^2}{\varepsilon_+ - \varepsilon_\infty}, \quad \beta^2 = \frac{\varepsilon_+\sigma^2 + \varepsilon_\infty\chi^2}{\varepsilon_+ - \varepsilon_\infty}.$$

For each given ε_+, ε_∞, and i the function $\chi_i(\sigma)$ generates a function β^2 of variable k^2. As an example at Fig. 3 we present the plot of the computed function $\beta^2 = \beta^2(k^2)$ corresponding to the fundamental mode (see the bottom curve plotted by the red solid line at Fig. 2) of the circular waveguide. Here, $\varepsilon_+ = 2$, $\varepsilon_\infty = 1$, and $i = 1$. Two points marked by circle and by square we will use in the next sections as test points for numerical solution of inverse spectral problems.

3.2 Inverse spectral problems

In this subsection we present three algorithms for approximate solution of three inverse spectral problems. The algorithms are based on the numerical solution of the nonlinear eigenvalue problem (16) for transverse wavenumbers. Namely, they are based on numerical calculations of characteristic values $\chi_1(\sigma)$ of the operator-valued function $A(\chi)$

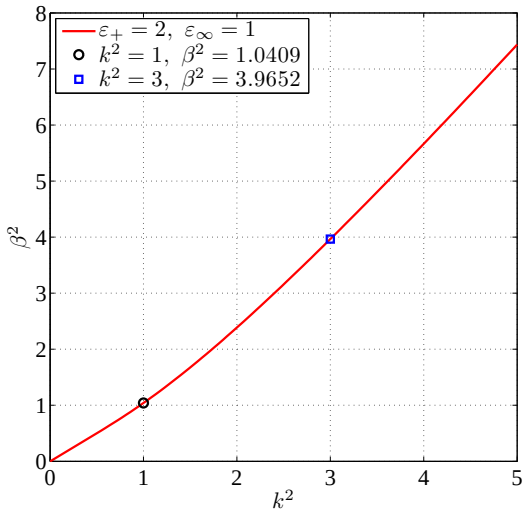

Figure 3: The red solid line is the plot of the computed function $\beta^2 = \beta^2(k^2)$ corresponding to the fundamental mode of the circular waveguide.

for fundamental mode and for σ in an appropriate interval. Note that the boundary γ of the waveguide's cross-section is given in all inverse problems.

3.2.1 Algorithm for reconstruction of the permittivity of the core

The first inverse problem is formulated as follows. Suppose that the permittivity ε_∞ of the cladding is given. Suppose that the propagation constant β of the fundamental mode is measured for a given wavenumber k. The measuring can be done by experimental methods described, for example, in [2]. It is necessary to calculate the permittivity ε_+ of the waveguide's core.

Inverse Eigenvalue Problem for the Permittivity of the Core (IEP-PCo). Given the information about the one natural fundamental eigenmode for k, β, and ε_∞ determine the unknown ε_+ such that $\varepsilon_+ > \varepsilon_\infty$ and belongs to the set of admissible parameters $\varepsilon_+ \in (\varepsilon_\infty, d_1]$ with a priori known constant $d_1 > \varepsilon_\infty$.

The solution of this inverse spectral problem is calculated by the following way.

Algorithm

- Step 1. Compute the number

$$\sigma = \sqrt{\beta^2 - k^2\varepsilon_\infty},$$

which is calculated for given values of β, k, and ε_∞.

- Step 2. Calculate the transverse wavenumber $\chi(\sigma)$ by the spline-collocation method for the obtained σ of the fundamental mode.

- Step 3. Compute the permittivity of the waveguide's core by the following explicit formula:
$$\varepsilon_+ = \frac{\chi^2 + \beta^2}{k^2}.$$

- Step 4. Put $\varepsilon_+ = d_1$, if computed at previous step $\varepsilon_+ > d_1$. Put $\varepsilon_+ = \varepsilon_\infty + d_2$, if computed $\varepsilon_+ \le \varepsilon_\infty$, where $d_2 > 0$ is a priori known constant.

We note that the transverse wavenumber $\chi(\sigma)$ in step 2 is calculated by an interpolation of the function $\chi_1(\sigma)$ with respect to the points obtained when the nonlinear spectral problem for transverse wavenumbers was numerically solved. Step 4 is similar to the formula (4.7) in [16].

3.2.2 Algorithm for reconstruction of the permittivity of the cladding

Suppose that the permittivity ε_+ of the core is given and that the propagation constant β of the fundamental mode is measured for a given wavenumber k. It is necessary to calculate the permittivity ε_∞ of the waveguide's cladding.

Inverse Eigenvalue Problem for the Permittivity of the Cladding (IEP-PCl). Given the information about the one natural fundamental eigenmode for k, β, and ε_+ determine the unknown ε_∞ such that $\varepsilon_\infty \ge 1$ and belongs to the set of admissible parameters $\varepsilon_\infty \in [1, \varepsilon_+)$.

The solution of this problem is calculated by the following algorithm.

Algorithm

- Step 1. Compute the number
$$\chi = \sqrt{k^2\varepsilon_+ - \beta^2}$$
which is calculated for given values of β, k and ε_+.

- Step 2. Calculate the transverse wavenumber σ by the spline-collocation method for the obtained χ for the fundamental mode.

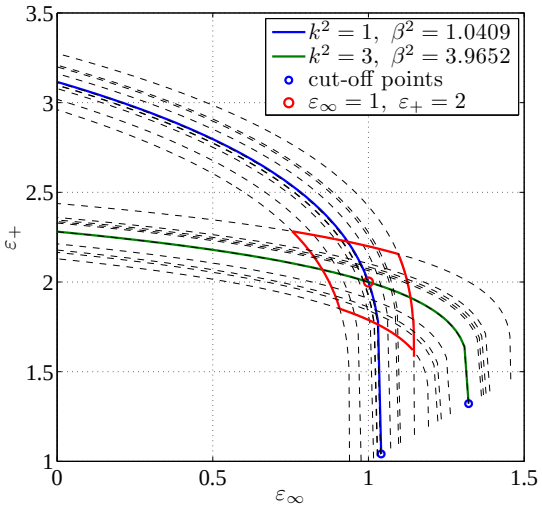

Figure 4: The blue and the green solid lines are plots of function $\varepsilon_+ = \varepsilon_+(\varepsilon_\infty)$ for given pairs of k and β for the fundamental mode of the circular waveguide. The unique exact solution of the inverse spectral problem is marked by the red circle. The approximate solution obtained by the spline-collocation method coincides with the red circle for the exact β. For randomly noised $\widetilde{\beta}$ approximate solutions are intersections of dashed lines. They belong to the red rhomb.

- Step 3. Compute the permittivity of the waveguide's cladding by the following explicit formula:
$$\varepsilon_\infty = \frac{\beta^2 - \sigma^2}{k^2}.$$

- Step 4. Put $\varepsilon_\infty = 1$, if computed at previous step $\varepsilon_\infty < 1$. Put $\varepsilon_\infty = \varepsilon_+ - d_3$, if computed $\varepsilon_\infty \ge \varepsilon_+$, where $d_3 > 0$ is a priori known constant.

3.2.3 Algorithm for reconstruction of both permittivities of the core and of the cladding

The full variant of our problem is the reconstruction of both permittivities of the core and of the cladding. The solution for the fundamental mode of nonlinear eigenvalue problem (16) for transverse wavenumbers gives us an implicit function ε_+ of the variable ε_∞ for each fixed longitudinal wavenumber k and propagation constant β. For example, at Fig. 4 the blue and the green solid lines are plots of this function for given pairs of k and β.

The intersection of this lines marked by the red circle is the unique exact solution of our problem. Therefore, we calculate the permittivities ε_+ and ε_∞ as the solution of the following nonlinear system of two equations:

$$\begin{cases} \chi(\sqrt{\beta_1^2 - k_1^2\varepsilon_\infty}) = \sqrt{k_1^2\varepsilon_+ - \beta_1^2}, \\ \chi(\sqrt{\beta_2^2 - k_2^2\varepsilon_\infty}) = \sqrt{k_2^2\varepsilon_+ - \beta_2^2}. \end{cases} \tag{21}$$

Here, k_1 and k_2 are some given distinct longitudinal wavenumbers, β_1 and β_2 are corresponding measured propagation constants; χ is the function of variable ε_∞ for fixed k_j and β_j, where $j = 1, 2$. The functions $\chi\left(\sqrt{\beta_j^2 - k_j^2\varepsilon_\infty}\right)$, $j = 1, 2$, of variable ε_∞ in (21) are calculated by an interpolation of the function $\chi_1(\sigma)$, where $\sigma = \sqrt{\beta_j^2 - k_j^2\varepsilon_\infty}$, for the fundamental mode (see the bottom curve plotted by the red solid line at Fig. 2).

Inverse Eigenvalue Problem for the Permittivities of the Core and the Cladding (IEP-PCoCl). Given the information about the two natural fundamental eigenmodes for longitudinal wavenumbers k_1 and $k_2 \neq k_1$ and corresponding β_1 and β_2 determine the unknown ε_+ and ε_∞ such that $\varepsilon_+ > \varepsilon_\infty$ and belongs to the set of admissible parameters $\varepsilon_+ \in (\varepsilon_\infty, d_1)$ with a priori known constant d_1 and $\varepsilon_\infty \in [1, \varepsilon_+)$.

Algorithm

- Step 1. Solve numerically nonlinear system of two equations (21) depending on two variables ε_+, ε_∞ for given numbers k_1, k_2, β_1, and β_2.
- Step 2. Put $\varepsilon_+ = d_1$, if computed at previous step $\varepsilon_+ > d_1$. Put $\varepsilon_\infty = 1$, if computed at previous step $\varepsilon_\infty < 1$. Put $\varepsilon_+ = \varepsilon_\infty + d_2$, if computed $\varepsilon_+ \leq \varepsilon_\infty$, where $d_2 > 0$ is a priori known constant.

3.3 Numerical results

Let us describe results of numerical experiments with core's permittivity reconstructions by the algorithm of subsection 3.2.1.

The mathematical analysis of existence of the solution of the original spectral problem (4)–(6) for transverse wavenumbers is presented in Theorems 1 and 2. The results of Theorems 1 and 2 are true for arbitrarily shaped waveguides. An illustration of the theoretical results is shown at Fig. 2 for a waveguide of circular cross-section. Analyzing Fig. 2 we observe that the fundamental mode

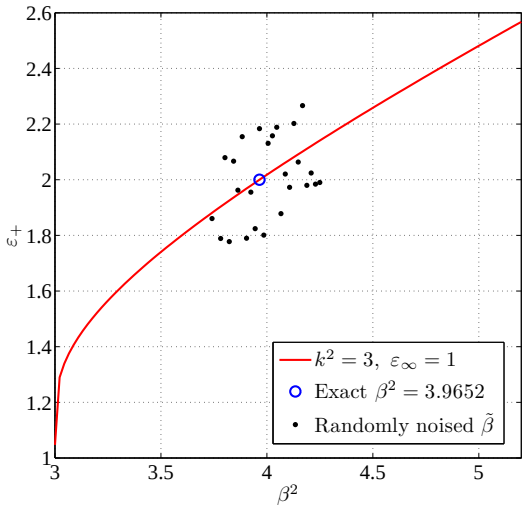

Figure 5: The red solid line is the plot of function $\varepsilon_+ = \varepsilon_+(\beta^2)$ for the fundamental mode of the circular waveguide. The approximate solution obtained by the spline-collocation method is marked by the blue circle for the exact β and by black points for the randomly noised $\widetilde{\beta}$.

(see the red solid curve at Fig. 2) exists for each wavenumber $k > 0$. The fundamental mode is unique, its dispersion curve does not intersect with any others curves and well separated from them. Therefore, the inverse spectral problem's solution exists and unique for each wavenumber $k > 0$, this solution depends continuously on given data. In other words, the inverse spectral problem is well-posed by Hadamard.

An example of this continuity dependence we can see at Fig. 5. The red solid line is the plot of the function ε_+ of β^2 for the fundamental mode.

In our computations by analogy with [17] we have introduced a randomly distributed noise in the propagation constant as

$$\widetilde{\beta} = \beta(1 + p\alpha),$$

where $\beta = \sqrt{3.9652}$ is the exact measured propagation constant, $\alpha \in (-1, 1)$ are randomly distributed numbers, and p is the noise level. In our computations we have used $p = 0.05$ and thus, the noise level was 5%.

Some numerical results of reconstruction of ε_+ are presented at Fig. 5. The approximated value $\varepsilon_{+,comp}$ of ε_+ for the noise-free data is marked at Fig. 5 by the blue circle. Approximated values

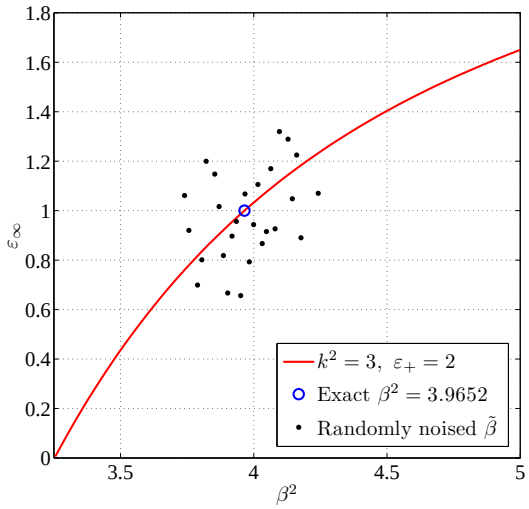

Figure 6: The red solid line is the plot of function $\varepsilon_\infty = \varepsilon_\infty(\beta^2)$ for the fundamental mode of the circular waveguide. The approximate solution obtained by the spline-collocation method is marked by the blue circle for the exact β and by black points for the randomly noised $\widetilde{\beta}$.

$\varepsilon_{+,comp}$ of ε_+ for randomly distributed noise $\widetilde{\beta}$ with the 5% noise level is marked at Fig. 5 by the black points. Using this figure we observe that the approximate solutions even for the randomly noised $\widetilde{\beta}$ were stable. The relative L_2 error $e = \frac{||\varepsilon_+ - \varepsilon_{+,comp}||}{||\varepsilon_+||}$ is on the interval $[0, 0.14]$, and approximated values $\varepsilon_{+,comp}$ differs from the exact values of ε_+ not more than 12%. We see that for the unique and stable reconstruction of the constant waveguide permittivity ε_+ it is enough to measure the propagation constant β of the fundamental mode for only one wavenumber k.

Note that in this numerical experiment all the approximated values $\varepsilon_{+,comp}$ of ε_+ for the noised data belong to the set of admissible parameters $\varepsilon_+ \in (\varepsilon_\infty, d_1)$ for $d_1 = 2.4$.

Analogous results we obtained for cladding's permittivity reconstructions by the algorithm described in subsection 3.2.2. As at the previous figure the red solid line at Fig. 6 is the plot of continuous function ε_∞ of squared β for the fundamental mode. The approximate solution $\varepsilon_{\infty,comp}$ obtained by the spline-collocation method is marked by the blue circle for the exact β and by black points for the randomly noised $\widetilde{\beta}$. Using this figure we observe that the approximate solutions for the randomly noised $\widetilde{\beta}$ were stable in this case too. The relative L_2 error of the reconstruction $e = \frac{||\varepsilon_\infty - \varepsilon_{\infty,comp}||}{||\varepsilon_\infty||}$ belongs approximatelly to the interval $[0, 0.67]$. Approximated values $\varepsilon_{\infty,comp}$ differs from the exact values of ε_∞ not more than 40%. We can conclude, that for the unique and stable reconstruction of the constant permittivity ε_∞ it is enough to measure the propagation constant β of the fundamental mode for only one wavenumber k.

Note that in this numerical experiment the exact solution ε_∞ belongs to the low boundary of the set of admissible parameters $\varepsilon_\infty \in [1, \varepsilon_+)$. Therefore a half of approximate solutions $\varepsilon_{\infty,comp}$ obtained for the randomly noised $\widetilde{\beta}$ are less than one. Then in the fourth step of the algorithm of section 3.2.2, we assign $\varepsilon_{\infty,comp} = 1$.

We finished our numerical experiments with full permittivity reconstructions by the algorithm described in subsection 3.2.3. The approximate solution obtained by the spline-collocation method is marked at Fig. 4 by the red circle for the exact propagation constant. We have also introduced the random noise in the propagation constant as we described above. The approximate solutions for the noised $\widetilde{\beta}$ are intersections of dashed lines. We see that the approximate solutions for the randomly noised $\tilde{\beta}$ belong to the red rhomb and are stable. Therefore, for the unique and stable reconstruction of the dielectric constants ε_∞ and ε_+ it is enough to measure the propagation constant β of the fundamental mode for two distinct wavenumbers k.

Note that in this numerical experiment all the approximated values $\varepsilon_{+,comp}$ of ε_+ for the noised data belong to the set of admissible parameters $\varepsilon_+ \in (\varepsilon_\infty, d_1)$ for $d_1 = 2.4$. Since $\varepsilon_\infty = 1$ a half of approximate solutions $\varepsilon_{\infty,comp}$ obtained for the randomly noised $\widetilde{\beta}$ are less than one. For these cases in the second step of the algorithm of section 3.2.3, we assign $\varepsilon_{\infty,comp} = 1$.

4 Parallel computing

In this section we describe in details the method of calculation of initial approximations to nonlinear eigenvalues. We consider a more complicated problem [6] on surface and leaky modes of optical fibers. Only surface modes satisfy to original problem (4)–(6). For leaky modes propagation constants β are complex. Hence transverse wavenumbers are complex too. As in previous sections de-

note by $\chi = \sqrt{k^2\varepsilon_+ - \beta^2}$ the (complex) transverse wavenumber in the core. But it is more convenient to denote the complex transverse wavenumber in the cladding by $\eta = \sqrt{k^2\varepsilon_\infty - \beta^2}$. Then equation (5) has the form

$$\Delta u + \eta^2 u = 0, \quad x \in \Omega_e. \tag{22}$$

Suppose that the domain Ω_i is a subset of a circle with radius R_0, then the function u satisfies to the Reichardt condition at infinity [10]:

$$u(r,\varphi) = \sum_{l=-\infty}^{\infty} a_l H_l^{(1)}(\eta r)\, e^{il\varphi}, \quad r \geq R_0. \tag{23}$$

The series in (23) should converge uniformly and absolutely.

For surface modes $\eta = i\sigma$, where $\sigma > 0$, and Reichardt condition (23) is equal [10] to condition of exponential decay (7). For leaky modes η is complex and $\mathrm{Im}(\chi) < 0$. Therefore, as it was shown in [10], Reichardt condition permits the fields to grow exponentially with $r \to \infty$. Nevertheless, results similar to Theorems 1-3 are true. These results were obtained in [6] and [11]. In [6] we used the representation of eigenfunctions of problem (4), (22), (6), (23) in the form of single-layer potentials (8) and

$$u(x) = \int_\gamma \Psi(\eta; x, y) g(y) dl(y), \quad x \in \Omega_e, \tag{24}$$

where

$$\Psi(\eta; x, y) = \frac{i}{4} H_0^{(1)}(\eta\,|x - y|). \tag{25}$$

In [11] we studied functions η_i of normalized and squared frequency $\lambda = k^2(\varepsilon_+ - \varepsilon_\infty) > 0$.

Using spline-collocation method in [8] we approximated problem (4), (22), (6), (23) by a nonlinear finite-dimensional eigenvalue problem of the form

$$A(\lambda, \eta) w = 0. \tag{26}$$

To obtain good initial approximations to complex nonlinear eigenvalues η for given values of parameter λ we investigate spectral properties of the matrix A as a function of variables η and λ. For each given point in an investigated domain of parameters η and λ we calculate the condition number of matrix A. Condition number is calculated by SVD method.

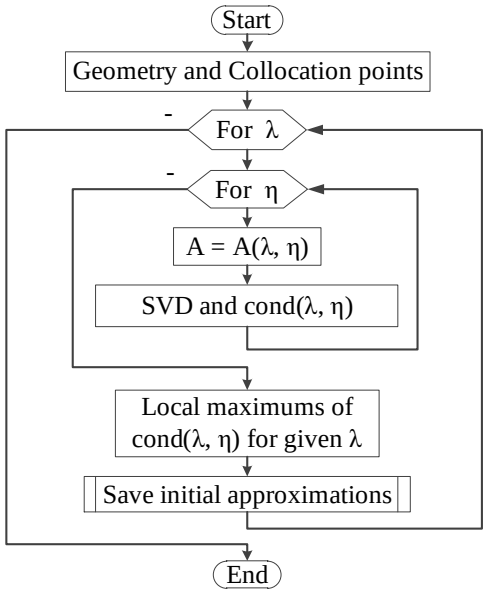

Figure 7: The sequential algorithm for numerical calculations of local maximums of condition number $\mathrm{cond}(\lambda, \eta) := \mathrm{cond}(A(\lambda, \eta))$ as a function of variables λ and η.

4.1 Sequential algorithm

In this subsection we present our basic sequential algorithm for calculations of local maximums of condition number as a function of variables λ and η. Recall that λ is positive; η is complex for leaky waves and pure imaginary for surface waves.

The first step is the definition of the waveguide's geometry and calculations of collocation points (see Fig. 7). The loop for λ is basic. For each given λ we make calculations in the inner loop for η. For given λ and η we calculate the matrix A. Then we make SVD and calculate $\mathrm{cond}(A(\lambda, \eta))$. The next step for given λ is numerical calculations of local maximums of condition number as a function of variable η. Finally for each given λ we save local maximums of condition number as initial approximations for nonlinear eigenvalues η.

4.2 Parallel algorithm

In this subsection we present a parallel modification of our basic algorithm for calculations of local maximums of condition number as a function of variables λ and η. We program for APK-1M compact supercomputer using C language. It is a cluster with two computational nodes. It has eight processors. Each computational node has four pro-

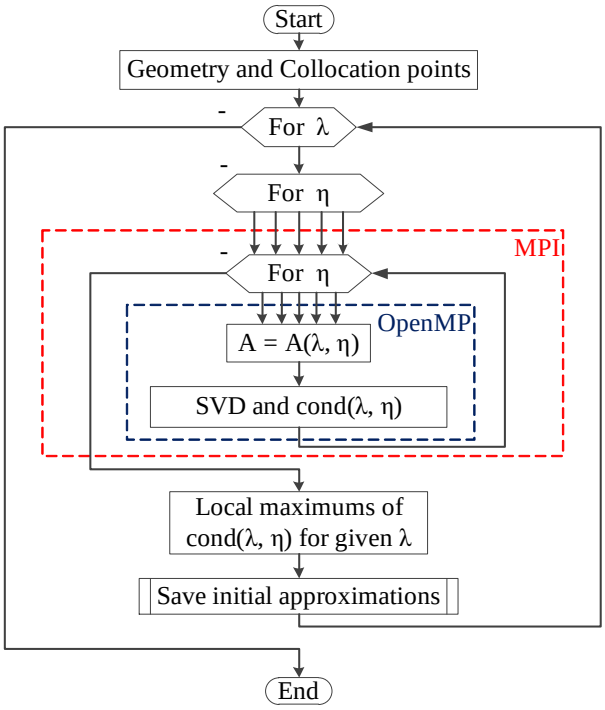

Figure 8: The parallel algorithm for numerical calculations of local maximums of condition number $\mathrm{cond}(\lambda, \eta) := \mathrm{cond}(A(\lambda, \eta))$ as a function of variables λ and η.

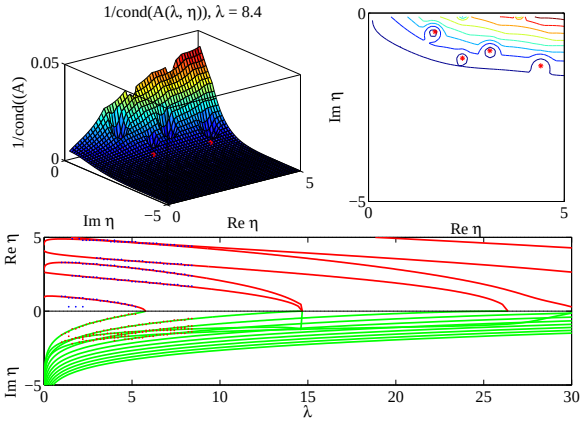

Figure 9: Initial approximations to nonlinear eigenvalues η for a waveguide of the circular cross-section for given λ.

cessors. Each processor quadruple share a half of all main memory. The main memory is uniformly distributed for two computational nodes. Thus, we use both MPI and OpenMP technologies. Message Passing Interface (MPI) is a technology for multiprocessor systems with distributed memory [18]. Open Multi-Processing (OpenMP) is a technology for computers with shared memory [19].

The loop of λ is sequential (see Fig. 8) because we want to make parallel computations for any specified λ. Hence we parallelize our algorithm for variable η. Firstly, we divide the computational domain of η for four or for eight subdomains according to the number of using processors. At this level of parallelization we use MPI. Secondly, we divide each subdomain of variable η for a fixed number of subsubdomains according to the number of OpenMP threads. We use OpenMP also for parallel computations of entries of the matrix A and for singular value decomposition.

Let us describe as how we use some functions of MPI. We use `MPI_Bcast` to dispatch the variables n, m, and λ to all processes:

```
MPI_Bcast(&n,1,MPI_INT,0,MPI_COMM_WORLD);
MPI_Bcast(&m,1,MPI_INT,0,MPI_COMM_WORLD);
MPI_Bcast(&lambda,1,MPI_DOUBLE,0,
    MPI_COMM_WORLD);
```

Note here, that n is the number of collocation points, m is the number of nodes in the meshed subdomain of η for each process. Then we use `MPI_Scatter` to scatter meshed subdomains of the variable η for all processes:

```
MPI_Scatter(re_chi,m,MPI_DOUBLE,
    local_re_chi,m,MPI_DOUBLE,0,
    MPI_COMM_WORLD);
MPI_Scatter(im_chi,m,MPI_DOUBLE,
    local_im_chi,m,MPI_DOUBLE,0,
    MPI_COMM_WORLD);
```

Finally, we use `MPI_Gather` to gather computed condition numbers in one array from all processes:

```
MPI_Gather(local_condition,m,MPI_DOUBLE,
    condition,m,MPI_DOUBLE,0,
    MPI_COMM_WORLD);
```

Each process runs on its own processor. Each processor has sixteen computational cores with shared cash memory. For parallel computations on each processor we use sixteen OpenMP threads for each process. We use the following OpenMP directive for loops of variable η:

```
#pragma omp parallel for private(i)
    for(i = 0; i < m; i++)
    {
```

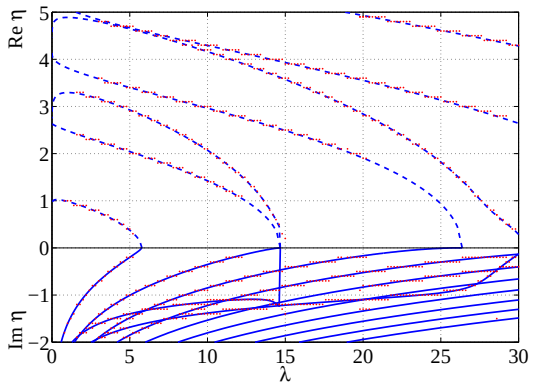

Figure 10: Initial approximations to complex eigenvalues η satisfying to leaky eigenwaves for a waveguide of the circular cross-section. The exact solution is plotted by solid lines (for Imη) and by dashed lines (for Reη). SVD results are marked by squares.

```
    int idxThread = omp_get_thread_num();
        ...
}
```

To control the sub-subdomain of η which was dedicated to the thread and to control the special memory array which was dedicated to the thread we use the function `omp_get_thread_num()`. This function returns the number of the thread. We also use `#pragma omp parallel for` directive for loops of indexes of matrix elements and for loops in SVD.

4.3 The comparison of computational technologies and hardware

We started our numerical experiments using a home personal computer with Intel Core i7 processor (2.90 GHz, 4 physical cores). We fixed $\lambda = 10$ and meshed the domain of the variable η by a 20-by-20 mesh: Re$\eta = 0 : 0.25 : 5$, Im$\eta = -5 : 0.25 : 0$. In these experiments the number n of collocation points was equal to 100. The results are presented in the following table:

Computational technologies	Time (sec.)
C	162
C+OpenMP(A)	95
C+OpenMP(η)	46
C+OpenMP(η)+OpenMP(A)	42

In this table we compare the time of computation for different computational technologies:

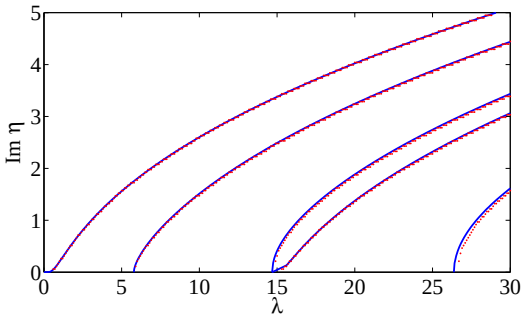

Figure 11: Initial approximations to pure imaginary eigenvalues η satisfying to surface eigenwaves for a waveguide of the circular cross-section. The exact solution is plotted by solid lines. SVD results are marked by squares.

- for the usual C sequential program,
- for parallel computing for elements of A,
- for parallel computing on the mesh of η,
- for parallel computing for matrix elements and on the mesh of η.

We see that the last parallel program works four times faster than the sequential program.

Our numerical experiments we continued using APK-1M. The abbreviation means a modification of the first hardware-software complex. Let us describe some characteristics of the compact supercomputer APK-1M:

- the peak performance is 1.075 TFlops,
- the main memory is 1024 GB,
- the disc storage is 18 TB.

As we have told, it is a cluster with two computational nodes based on the motherboards H8QG6-F. Each computational node has four processors AMD Opteron 6272 with sixteen computational cores. Therefore, one computational node has 64 cores.

For numerical experiments with supercomputer we fixed $\lambda = 10$ and meshed the domain of the variable η by a 48-by-48 mesh: Re$\eta = 0 : 0.104 : 5$, Im$\eta = -5 : 0.104 : 0$. The results for $n = 100$ are presented in this table:

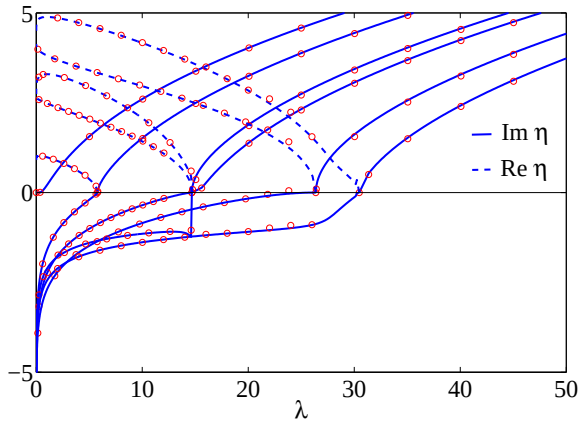

Figure 12: Dispersion curves for surface and leaky eigenwaves of the circular waveguide. The exact solution is plotted by solid lines and by dashed lines. The numerical solutions obtained by the residual inverse iteration method are marked by circles.

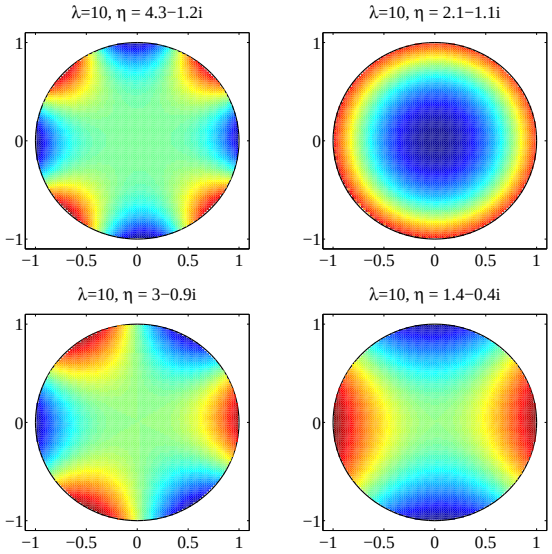

Figure 13: Isolines for leaky eigenwaves of the circular waveguide.

Computational technologies and hardware	Time (sec.)	Processors	MPI proc.	OMP threads
PC: OpenMP	390	1	-	8
APK-1M: OpenMP	78	4	-	64
APK-1M: OpenMP+ MPI (1CN)	78	4	4	64

We compare the time of computations for different computational technologies and hardware:

- for OpenMp computations using a home PC with Intel Core i7 processor,
- for the same computations using APK-1M,
- for OPenMP and MPI computations using APK-1M as we described in previous section.

We see that parallel programs for APK-1M work five times faster than the OpenMp program for home PC. Note here, that we used only one computational node for these experiments. If we use two nodes then supercomputer works ten times faster than home PC.

4.4 Numerical results

In this subsection we describe some numerical results for the 48-by-48 mesh of complex η and for a 150-nodes mesh of positive λ. The figures presented at Fig. 9 were animated by the changing of λ. Fig. 9 shows a frame for $\lambda = 8.4$ of this movie. At the upper left corner of the figure we present the surface of the inverse condition number function of complex variable η. At the upper right corner we present the isolines of this function. At the bottom of this figure we present initial approximations to nonlinear eigenvalues η for λ up to value 8.4.

At Fig. 10 we present initial approximations to nonlinear eigenvalues η for λ from 0 to 31. Complex eigenvalues η are satisfied to leaky eigenwaves. The numerical results were obtained for a dielectric waveguide of the circular cross-section. The exact solution for this case is well known [4]. So, we compare obtained numerical results with the exact solution. The exact solution is plotted by blue solid lines (for $\mathrm{Im}\,\eta$) and by blue dashed lines (for $\mathrm{Re}\,\eta$). SVD results are marked by small red squares. Note here, that squares are the initial approximations only. They are start points for inverse iterations which we use for numerical solution of the nonlinear eigenvalue problem.

At Fig. 14 we present initial approximations to pure imaginary eigenvalues η satisfying to surface eigenwaves. We compare numerical results with the exact solution for the circular waveguide. The exact solution is plotted by solid lines. SVD results are marked by squares. As at the previous figure the squares are the initial approximations only.

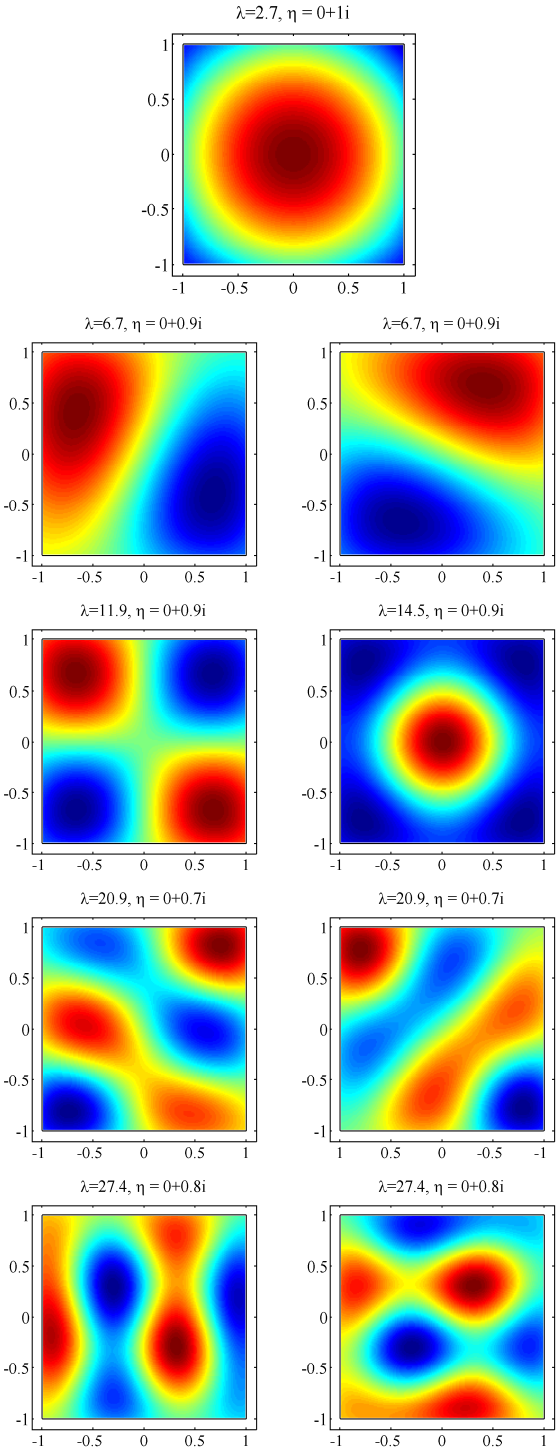

Figure 14: Isolines for surface eigenwaves of a weakly guiding dielectric waveguide of the square cross-section.

We used these initial approximations as start points for the residual inverse iteration method [14]. Using this iteration method for each given λ we solved numerically the nonlinear eigenvalue problem on eigenvalues η. At Fig. 12 we present some dispersion curves for surface and leaky eigenwaves of the circular waveguide. The exact solution is plotted by solid lines and by dashed lines. The numerical solutions obtained by the residual inverse iteration method are marked by circles. At Figs. 13 and 14 we present some isolines for leaky eigenwaves of the circular waveguide and for surface eigenwaves of the square waveguide.

5 Conclusion

In this work we showed that our three inverse spectral problems are well-posed. It is important to note that any information on specific values of eigenfunctions is not required. For solution of these inverse problems it is enough to know that the fundamental mode is excited, and then to measure its propagation constant for one or for two frequencies.

This approach satisfies to the practice of physical experiments because usually the fundamental mode is excited for practical purposes. Moreover, the fundamental mode can be excited only for the enough wide interval of frequencies.

For the approximate solution of the inverse problems we propose first to solve the nonlinear spectral problem for transverse wavenumbers in order to compute the dispersion curve for the fundamental mode. These calculations are done accurately by the spline-collocation method. Next, we uniquely and stably reconstruct the permittivities in our inverse algorithms.

Numerical experiments showed practical effectiveness of our approach to use SVD of the matrix for spline-collocation method for numerical calculations of initial approximations to nonlinear eigenvalues. Because of our numerical tests we can conclude that our software package can be used for numerical simulations of new type's optical fibers and for numerical reconstructions of dielectric constants of optical fibers on APK-1M supercomputer.

Acknowledgements

The authors would like to thank Michael Havrilla and George Hanson for helpful discussions concerning the topics covered in this work.

This work was funded by the subsidy allocated to Kazan Federal University for the state assignment in the sphere of scientific activities; the work was supported also by RFBR and by Government of Republic Tatarstan, grant 12-01-97012-r_povolzh'e_a. The research of Larisa Beilina was supported by the Swedish Research Council, the Swedish Foundation for Strategic Research (SSF) through the Gothenburg Mathematical Modelling Centre (GMMC) and by the Swedish Institute, Visby Program.

References

[1] Havrilla, M., Bogle, A., Hyde IV, M., Rothwell, E., 2014, EM material characterization of conductor backed media using a NDE microstrip probe, *Studies in Applied Electromagnetics and Mechanics*. Vol. **38**, No. 2, pp. 210-218.

[2] Janezic, M.D., Jargon, J.A., 1999, Complex permittivity determination from propagation constant measurements, *IEEE Microwave and Guided Wave Letters*. Vol. **9**, No. 2, pp. 76–78.

[3] Chu, M.T., Golub, G.H., 2005, Inverce Eigenvalue Problems: Theory, Algorithms, and Applications. Oxford University Press.

[4] Snyder, A.W., Love, J.D., 1983, Optical Waveguide Theory. Chapman and Hall, London.

[5] Karchevskii, E.M., 1998, Study of spectrum of guided waves of dielectric fibers, *Mathematical Methods in Electromagnetic Theory, MMET 98, Conference Proceedings*. Vol. 2, pp. 787–788.

[6] Karchevskii, E.M., 1999, Analysis of the eigenmode spectra of dielectric waveguides, *Computational Mathematics and Mathematical Physics*. Vol. **39**, No. 9, pp. 1493–1498.

[7] Karchevskii, E.M., 2000, The fundamental wave problem for cylindrical dielectric waveguides. *Differential Equations*. Vol. **36**, No. 7, pp. 1109–1111.

[8] Spiridonov, A.O., Karchevskiy, E.M., 2013, Projection methods for computation of spectral characteristics of weakly guiding optical waveguides. *Proceedings of the International Conference Days on Diffraction 2013, DD 2013*, pp. 131–135.

[9] Karchevskii, E.M., Solov'ev, S.I., 2000, Investigation of a spectral problem for the Helmholtz operator on the plane. *Differential Equations*. Vol. **36**, No. 4, pp. 631–634.

[10] Kartchevski, E.M., Nosich, A.I., Hanson, G.W., 2005, Mathematical analysis of the generalized natural modes of an inhomogeneous optical fiber. *SIAM J. Appl. Math.* Vol. **65**, No. 6, pp. 2033–2048.

[11] Frolov, A., Kartchevskiy, E., 2013, Integral equation methods in optical waveguide theory. *Springer Proceedings in Mathematics and Statistics*. Vol. **52**, pp. 119–133.

[12] Karchevskiy, E., Shestopalov, Y., 2013, Mathematical and numerical analysis of dielectric waveguides by the integral equation method. *Progress in Electromagnetics Research Symposium, PIERS 2013 Stockholm, Proceedings*, pp. 388–393.

[13] Colton, D., Kress, R., 1983, Integral Equation Methods in Scattering Theory. Jhon Wiley and Sons, New York.

[14] Neumaier, A., 1985, Residual inverse iteration for the nonlinear eigenvalue problem. *SIAM J. Numer. Anal.* Vol. **22**, No. 5, pp. 914–923.

[15] Hua, Yingbo, Sarkar, Tapan K., 1991, On SVD for estimating generalized eigenvalues of singular matrix pencil in noise, *IEEE Transactions on Signal Processing* Vol. **39**, No. 4, pp. 892–900.

[16] Nguyen Trung Thanh, Beilina, L., Klibanov, M.V., Fiddy, M.A., 2014, Reconstruction of the refractive index from experimental backscattering data using a globally convergent inverse method. *SIAM J. Sci. Comput.*, Vol. **36**, No. 3, pp. B273–B293.

[17] Beilina, L., Klibanov, M.V., 2012, A new approximate mathematical model for global convergence for a coefficient inverse problem with backscattering data. *Inverse and Ill-Posed Problems*, Vol. **20**, pp. 513–565.

[18] Gropp, W., Lusk, E., Doss, N., Skjellum, A., 1996, A high-performance, portable implementation of the MPI message passing interface standard. *Parallel Computing*. Vol. **22**, No. 6, pp. 789–828.

[19] Yang, L.T., Guo, M., 2006, High-Performance Computing: Paradigm and Infrastructure, John Wiley & Sons, Inc.